

## Supplementary Data

### Supplementary Materials and Methods

#### *Protein S-nitrosylation detection by SNOB1 reagent*

To compare GluN2A and GluN1 S-nitrosylation levels in *Prnp*<sup>+/+</sup> and *Prnp*<sup>0/0</sup> hippocampi, we used the SNOB1 reagent (sc-361363; Santa Cruz Biotechnology, Dallas, TX). Two *Prnp*<sup>+/+</sup> and two *Prnp*<sup>0/0</sup> hippocampi were separately homogenized in 1 ml phosphate-buffered saline (PBS) + 0.5% Triton X-100 + protease inhibitors and centrifuged for 10 min at 5000 rpm at 4°C. Protein concentration in the supernatant was determined by bicinchoninic acid assay, and the same amount of protein was used as input for the following steps. Half of the protein extract was added to PBS + 0.5% Triton up to 1 ml and incubated with 0.5 mM SNOB1 for 30 min at 37°C in the dark according to the manufacturer's instructions. The second half of the sample was added to PBS + 0.5% Triton up to 1 ml and incubated with 0.5 mM biotin for 30 min at 37°C in the dark, as negative control. To purify SNOB1-bound proteins, 50  $\mu$ l of wet Immobilized NeutrAvidin Agarose (29200; ThermoFisher, Waltham, MA) were added to the samples and incubated for 2 h at room temperature (RT). Resin was washed five times PBS + 0.5% Triton. Then, proteins were eluted directly in SDS-PAGE sample buffer, boiled, and processed for Western blot detection. For each sample, 30  $\mu$ g of protein extract was loaded as input. The following primary antibodies were used: anti-GluN1 1:500–1:2000 (G8913; Sigma-Aldrich, St Louis, MO); anti-GluN2A 1:500–1:2000 (G9038; Sigma-Aldrich); anti- $\beta$ -actin peroxidase (AC-15) 1:10,000 (A3854; Sigma-Aldrich). After incubation with the secondary antibody, membranes were developed with the ECL detection reagent (GE Healthcare, Waukesha, WI) and recorded by the digital imaging system Alliance 4.7 (UVITEC, Cambridge, United Kingdom). Band quantification was performed with Uviband 15.0 software (UVITEC) obtaining an optical density (OD) value. To normalize OD values, the following formula was applied: (SNOB1-NMDAR subunit/input)/(SNOB1- $\beta$ -actin/input). Basically, S-nitrosylation signals were normalized on the corresponding input. Then, N-methyl-D-aspartate receptors (NMDAR) subunit values were normalized on  $\beta$ -actin value. *Prnp*<sup>+/+</sup> and *Prnp*<sup>0/0</sup> samples were compared by the Mann–Whitney test setting  $F(x) < G(x)$  as alternate hypothesis.

#### *Co-immunoprecipitation*

To compare GluN2A, GluN1, and neuronal nitric oxide synthase (nNOS) synaptic levels in *Prnp*<sup>+/+</sup> and *Prnp*<sup>0/0</sup> hippocampi, we performed a co-immunoprecipitation (coIP) with postsynaptic density protein 95 (PSD95). Samples from 6-, 10-, and 12-month-old male mice were used to parallel the biotin switch assay experiments, while postnatal day 20 (P20) mouse hippocampi were used to parallel organotypic hippocampal cultures (OHC) excitotoxicity studies. Samples were homogenized in 50 mM Tris-HCl, pH 7.5, 150 mM NaCl, 1 mM EDTA, 0.5% CHAPS, 10% glycerol, protease inhibitor cocktail, 5 mM NaF (S7920; Sigma-Aldrich), 0.5 mM Na<sub>3</sub>VO<sub>4</sub> (S6508; Sigma-Aldrich), protein concentration was evaluated by the BCA assay to use the same amount of proteins in each

sample. For PSD95 coIP with GluN2A (direct interaction) and GluN1 (indirect interaction), hippocampal protein extracts were precleared by 30 min incubation at 4°C with protein A/G (1:2) resin (17-5138-01 and 17-0618-01; GE Healthcare, Waukesha, WI). Then, the samples were incubated for 2.5 h at 4°C with 2  $\mu$ g/ml of either anti-PSD95 antibody (ab2723; Abcam, Cambridge, United Kingdom) or normal mouse IgG (mIgG, 12-371; Millipore, Billerica, MA), followed by 2 h incubation with protein A/G (1:2) resin. For nNOS coIP with PSD95, hippocampal protein extracts were incubated O/N at 4°C with 2  $\mu$ g/ml of either anti-nNOS antibody (4234; Cell Signaling, Danvers, MA) or normal rabbit IgG (rIgG, 12-370; Millipore), followed by 2 h incubation with protein A/G (1:2) resin. Proteins eluted from the resin were processed for standard Western blot protocol and revealed with anti-GluN1 1:2000 (G8913; Sigma-Aldrich), anti-GluN2A 1:2000 (G9038; Sigma-Aldrich), anti-nNOS, anti-PrP SHA31 1  $\mu$ g/ml (A03213; BertinPharma, Montigny le Bretonneux, France), and anti-PSD95 antibodies. After incubation with the secondary antibody, membranes were developed with the ECL detection reagent (GE Healthcare) and recorded by Alliance 4.7 digital imaging system (UVITEC). Band quantification was performed with Uviband 15.0 software (UVITEC) obtaining an OD value. To normalize OD values, the following formula was applied: (co-immunoprecipitated protein/input)/(immunoprecipitated protein/input), that is, [GluN2A (or GluN1) coIP/input]/[PSD95 IP/input] and (PSD95 coIP/input)/(nNOS IP/input). Then, *Prnp*<sup>+/+</sup> and *Prnp*<sup>0/0</sup> samples were compared by the Mann–Whitney test setting  $F(x) < G(x)$  as alternate hypothesis.

#### *NADPH consumption assay*

To estimate *Prnp*<sup>+/+</sup> and *Prnp*<sup>0/0</sup> nNOS activity level, we evaluated the kinetics of NADPH consumption. Samples from 6-month-old and P20 male mice were used to parallel the biotin switch assay experiments and OHC excitotoxicity studies, respectively. Samples were homogenized in 30 mM Tris-HCl, pH 7.5, and protease inhibitor cocktail and centrifuged at 10,000 g; the supernatant was used for the assay. The protein concentration was evaluated by the BCA assay to use the same amount of proteins in each sample (~1 mg). Five mM NADPH (481973; Millipore) was prepared in ddH<sub>2</sub>O and added to each sample to 0.5 mM final concentration. The kinetics of NADPH consumption was evaluated by measuring the absorbance at 340 nm each minute for 30 min. For each sample, the respective absorbance without NADPH addition was subtracted as blank to avoid differences in tissue scattering.

#### *NOS activity assay*

To measure *Prnp*<sup>+/+</sup> and *Prnp*<sup>0/0</sup> NOS activity level, we used the NOS activity assay kit (Item Number 781001; Cayman, Ann Arbor, MI). Samples from 6-month-old and P20 male mice were used to parallel the biotin switch assay experiments and OHC excitotoxicity studies, respectively. We used the radiolabeled substrate [<sup>3</sup>H]Arginine monohydrochloride (40–70 Ci/mmol, 1  $\mu$ Ci/ $\mu$ l [Item

No. NET1123001MC; Perkin Elmer, Waltham, MA]). The assay was run according to the manufacturer's instructions. Results are reported as counts per minute (cpm) subtracted of the blank-corresponding cpm value. As control of the specificity of the assay for the NOS activity, we measured the conversion of radiolabeled arginine in radiolabeled citrulline in the presence of the NOS blocker *N* $\omega$ -nitro-L-arginine (NNA, N5501; Sigma-Aldrich).

#### *MTT mitochondrial toxicity assay*

To evaluate the early phase of change in neuronal cell viability, the MTT (Thiazolyl Blue Tetrazolium Bromide) mitochondrial toxicity assay was performed on OHC after exposure to an excitotoxic stimulus. The MTT assay was set up following the protocol by Mazzone (1) with a few modifications. A 5 mg/ml MTT (M5655; Sigma-Aldrich) stock solution was prepared in PBS, pH 7.4. After 13 days *in vitro*, *Prnp*<sup>+/+</sup> and *Prnp*<sup>0/0</sup> OHC were exposed to 5  $\mu$ M NMDA in serum-free medium for 3 h. After one wash, OHC were incubated with 0.5 mg/ml MTT in serum-free medium for 2 h at 37°C. To dissolve formazan crystals, OHC were incubated overnight at 37°C with 1 ml of acidified isopropanol (0.04 N HCl in isopropanol). Absorbance values were measured at 570 and 690 nm. The 690 nm absorbance value was used as background, hence subtracted to the 570 nm signal. Cell viability was expressed as percentage of the control OHC value that was considered to be 100% viable and compared by the Mann–Whitney test setting  $F(x) < > G(x)$  as alternate hypothesis.

#### *Primary cell culture preparation and measurement of relative intracellular $Ca^{2+}$ [ $Ca^{2+}$ ]<sub>i</sub> changes after NMDA and cuprizone treatment*

Primary cell cultures were prepared from wild-type mouse hippocampal neurons. Hippocampi were dissected from P1 rats in the presence of 100  $\mu$ M kynurenic acid and 25  $\mu$ M 2-amino-5-phosphonovaleric acid (Tocris Biosciences, Missouri, United Kingdom). The isolated tissue was quickly sliced and digested with trypsin in the presence of DNase. After stopping the digestion with trypsin inhib-

itor, cells were triturated in the dissection medium containing DNase. After centrifugation, the resuspended cell pellet was distributed to 24-well Nunc cell culture multidishes previously coated with polyornithine (0.5 mg/ml) and Matrigel (2% [w/v]; BD Biosciences, San Jose, CA), each one containing 0.5 ml of modified minimal essential medium supplemented with dialyzed fetal bovine serum (Gibco, Carlsbad, CA). Two days after plating, the culture medium was supplemented with 2.5  $\mu$ M Arabinosylcytosine (Sigma), which inhibits the growth of glial cells. The culture medium was exchanged every 2–3 days. The experiments were performed after 15 days *in vitro*. Primary culture neurons were washed, exposed to Fluo-3 AM (F-1242; Life Technologies, Carlsbad, CA), the dye indicator, for 60 min at 37°C, washed two times, equilibrated for 30 min at 22°C, and washed. [ $Ca^{2+}$ ]<sub>i</sub> levels were determined as described by Tauskela *et al.* with a few modifications (2) by using temperature-controlled plate reader (EnSpire; Perkin Elmer) to measure fluorescence intensity (excitation wavelength 488 nm; emission wavelength 526 nm). Fluorescence intensities were measured from 19 locations within each well before the treatment and 0, 5, 10, and 15 min after the treatment (control, 20  $\mu$ M cuprizone [CZ], 5  $\mu$ M NMDA, 5  $\mu$ M NMDA + 20  $\mu$ M CZ). The background intensity was measured in cell-free plate with dye-free buffer. The fold increase in [ $Ca^{2+}$ ]<sub>i</sub> levels was calculated by subtracting the background intensity and normalizing on the resting conditions in each well.

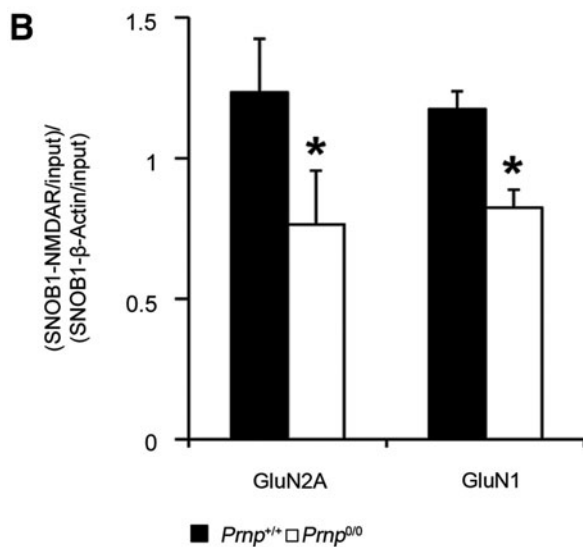
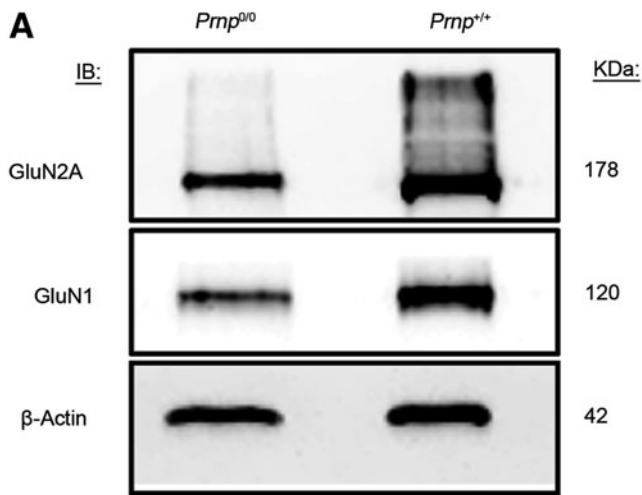
#### **Supplementary References**

1. Mazzone GL, Margaryan G, Kuzhandaivel A, Nasrabad SE, Mladinic M, and Nistri A. Kainate-induced delayed onset of excitotoxicity with functional loss unrelated to the extent of neuronal damage in the *in vitro* spinal cord. *Neuroscience* 168: 451–462, 2010.
2. Tauskela JS, Brunette E, O'Reilly N, Mealing G, Comas T, Gendron TF, Monette R, and Morley P. An alternative  $Ca^{2+}$ -dependent mechanism of neuroprotection by the metalloporphyrin class of superoxide dismutase mimetics. *FASEB J* 19: 1734–1736, 2005.

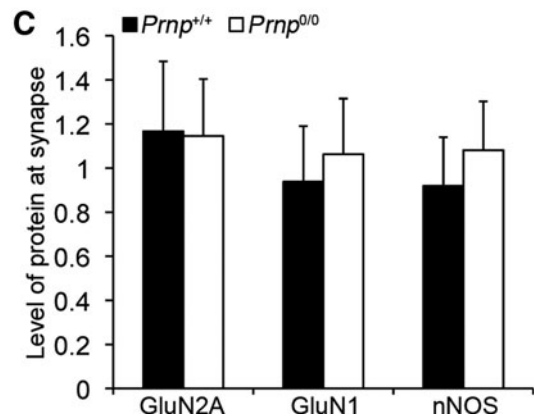
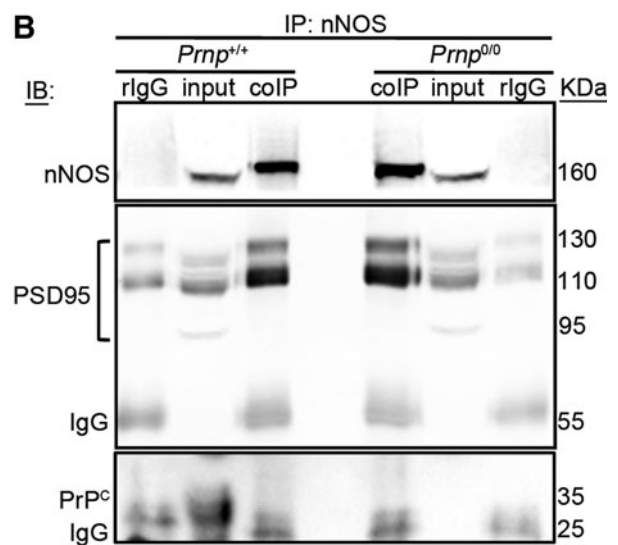
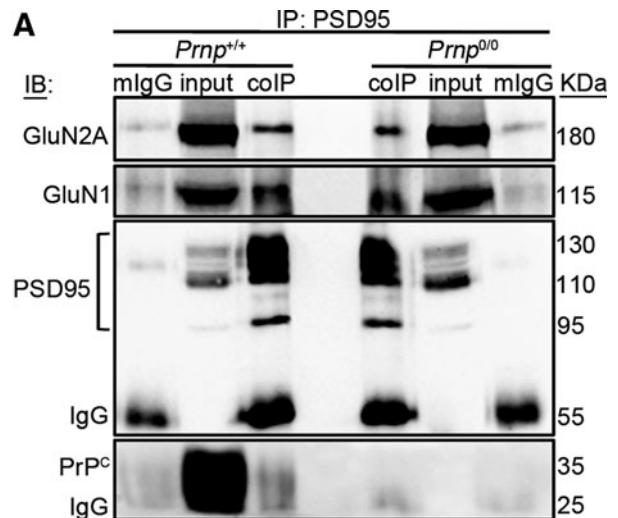
SUPPLEMENTARY TABLE S1. ORGANOTYPIC HIPPOCAMPAL CULTURE TREATMENTS

<i>Drug</i>	<i>Control</i>	<i>Pretreatment</i>	<i>Treatment</i>	<i>Washout (h)</i>
Excitotoxic stimulus				
5 $\mu$ M NMDA	ddH <sub>2</sub> O	—	10 min	24
10 $\mu$ M NMDA	ddH <sub>2</sub> O	—	3 h	24
Calcium chelation				
10 $\mu$ M NMDA + 2 mM EGTA	10 $\mu$ M NMDA; 2 mM EGTA; PBS pH 7.4	—	10 min	24
5 $\mu$ M NMDA + 2 mM EGTA	5 $\mu$ M NMDA; 2 mM EGTA; PBS pH 7.4	—	1.5 h	24
NMDA receptor inhibition				
5 $\mu$ M NMDA + 50 $\mu$ M AP5	5 $\mu$ M NMDA; 50 $\mu$ M AP5; ddH <sub>2</sub> O	30 min AP5	3 h	24
AMPA/kainate receptor inhibition				
5 $\mu$ M NMDA + 20 $\mu$ M CNQX	5 $\mu$ M NMDA; 20 $\mu$ M CNQX; 0.002% DMSO	30 min CNQX; 30 min 0.002% DMSO	3 h	24
GluN2B-containing NMDA receptor inhibition				
10 $\mu$ M NMDA + 3 $\mu$ M ifenprodil	10 $\mu$ M NMDA; 3 $\mu$ M ifenprodil; ddH <sub>2</sub> O	—	10 min	24
Copper chelation				
5 $\mu$ M NMDA + 20 $\mu$ M CZ	5 $\mu$ M NMDA; 20 $\mu$ M CZ; 50% EtOH	—	3 h	24
nNOS inhibition				
5 $\mu$ M NMDA + 1 mM NNA	5 $\mu$ M NMDA; 1 mM NNA	30 min 1 mM NNA	3 h	24
NO donor				
5 $\mu$ M NMDA + 20 $\mu$ M GSNO	5 $\mu$ M NMDA; 20 $\mu$ M GSNO; ddH <sub>2</sub> O	—	3 h	24

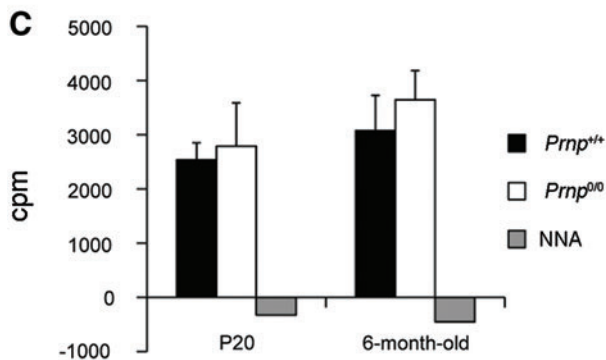
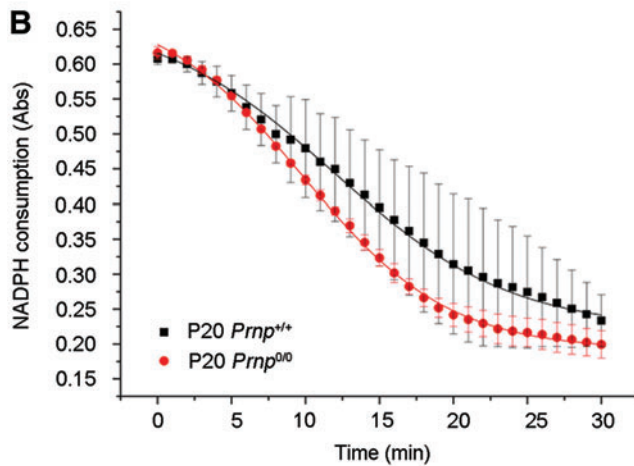
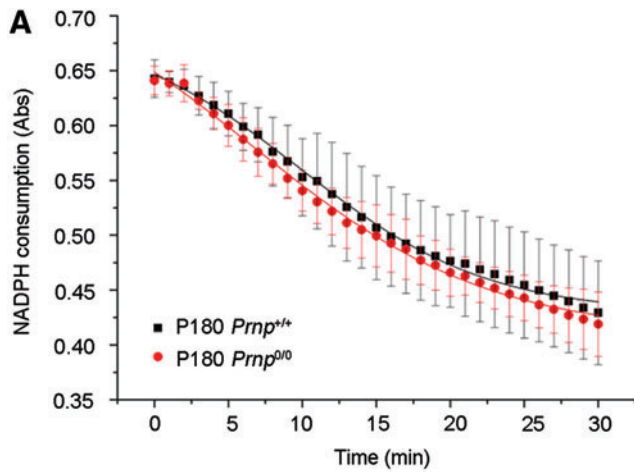
AMPA,  $\alpha$ -amino-3-hydroxy-5-methyl-4-isoxazolepropionic acid; AP5, (2*R*)-amino-5-phosphonovaleric acid; CNQX, 6-cyano-7-nitroquinoxaline-2,3-dione; CZ, cuprizone; DMSO, dimethyl sulfoxide; EGTA, ethylene glycol tetraacetic acid; EtOH, ethanol; GSNO, S-nitrosoglutathione.; NMDA, *N*-methyl-D-aspartate; NNA, *N* $\omega$ -nitro-L-arginine; nNOS, neuronal nitric oxide synthase; NO, nitric oxide; PBS, phosphate-buffered saline.



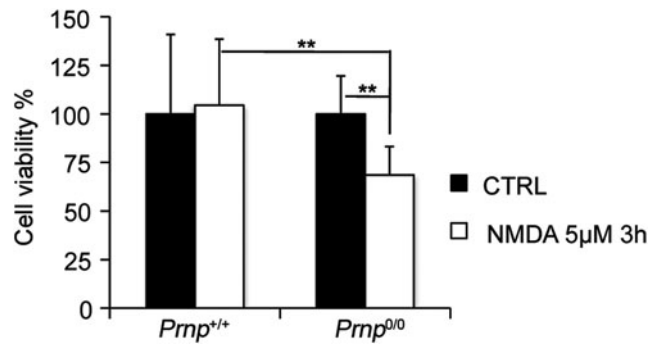
**SUPPLEMENTARY FIG. S1. NMDAR subunit S-nitrosylation levels comparison in wild-type and PrP<sup>C</sup> knockout hippocampi by SNOB1 reagent.** (A) Immunoblot signals corresponding to SNOB1-bound GluN2A, GluN1, and  $\beta$ -actin in *Prnp<sup>+/+</sup>* and *Prnp<sup>0/0</sup>* hippocampi. (B) Graph showing the quantification of the immunoblot signals normalized according to the following formula: (SNOB1-NMDAR subunit/input)/(SNOB1- $\beta$ -actin/input); all error bars indicate SD;  $n=4$ ; \* $p < 0.05$ . NMDAR, *N*-methyl-D-aspartate receptors.



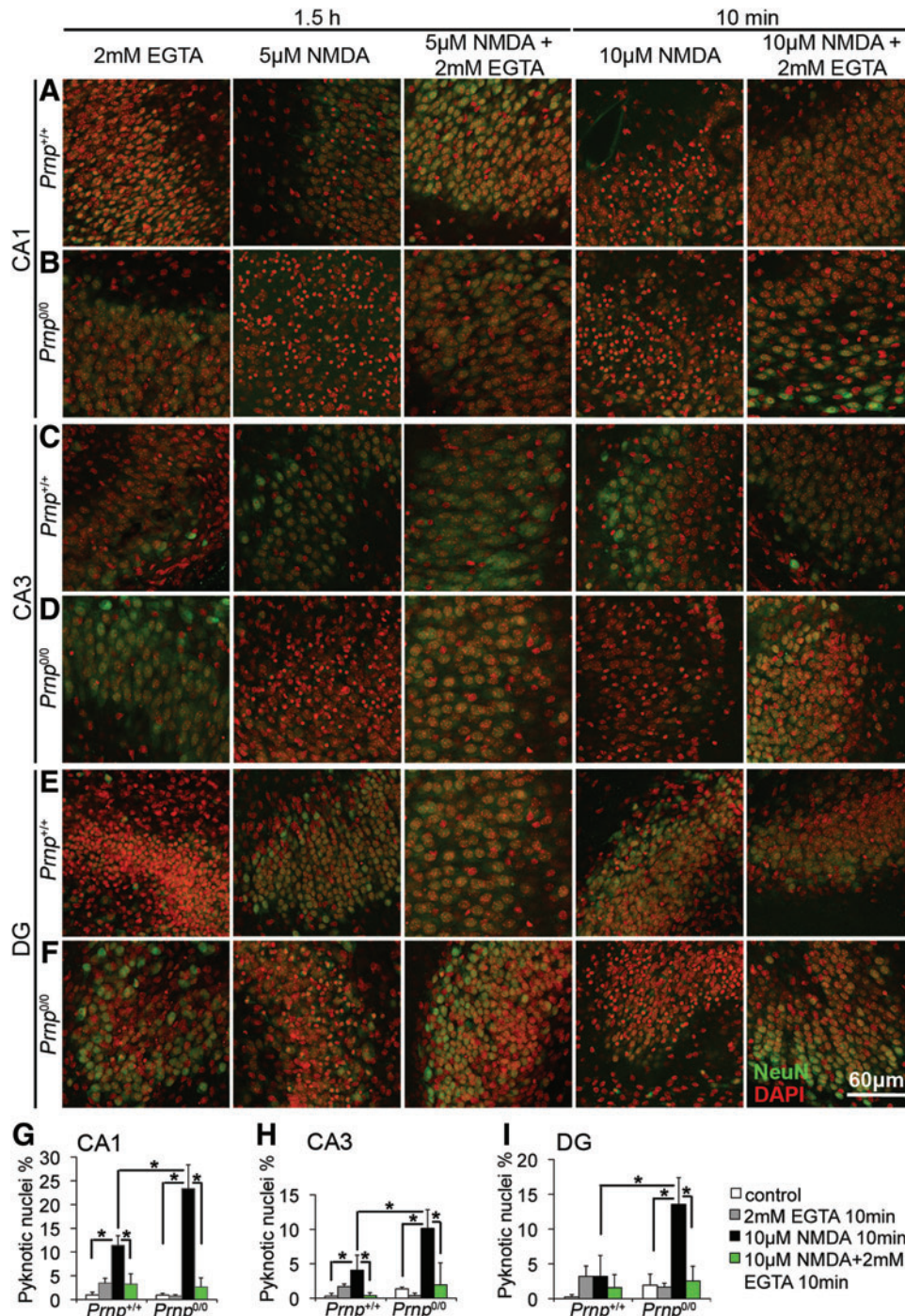
**SUPPLEMENTARY FIG. S2. CoIP of GluN2A and GluN1 with PSD95 and coIP of PSD95 with nNOS show comparable levels in adult *Prnp<sup>+/+</sup>* and *Prnp<sup>0/0</sup>* hippocampi.** (A) coIP of GluN2A and GluN1 with PSD95. (B) coIP of PSD95 with nNOS. (C) Graph showing the quantification of the coIP signals normalized according to the following formula: (co-immunoprecipitated protein/input)/(immunoprecipitated protein/input); all error bars indicate SD;  $n=3$ . coIP, co-immunoprecipitation; nNOS, neuronal nitric oxide synthase; PSD95, postsynaptic density protein 95.



**SUPPLEMENTARY FIG. S3. NADPH consumption assay and radiolabeled arginine conversion in citrulline shows comparable NOS activity levels in *Prnp*<sup>+/+</sup> and *Prnp*<sup>0/0</sup> mice.** (A) NADPH consumption assay in P180 *Prnp*<sup>+/+</sup> and *Prnp*<sup>0/0</sup> samples; (B) NADPH consumption assay in P20 *Prnp*<sup>+/+</sup> and *Prnp*<sup>0/0</sup> samples; all error bars indicate SD;  $n=3$ ; (C) radiolabeled citrulline level measurements in P20 and 6-month-old *Prnp*<sup>+/+</sup> and *Prnp*<sup>0/0</sup> mouse samples; all error bars indicate SD;  $n=4$ ; *black columns* correspond to *Prnp*<sup>+/+</sup> mice, *white columns* correspond to *Prnp*<sup>0/0</sup> mice, *gray columns* correspond to the control with NNA. NNA, *N* $\omega$ -nitro-L-arginine.

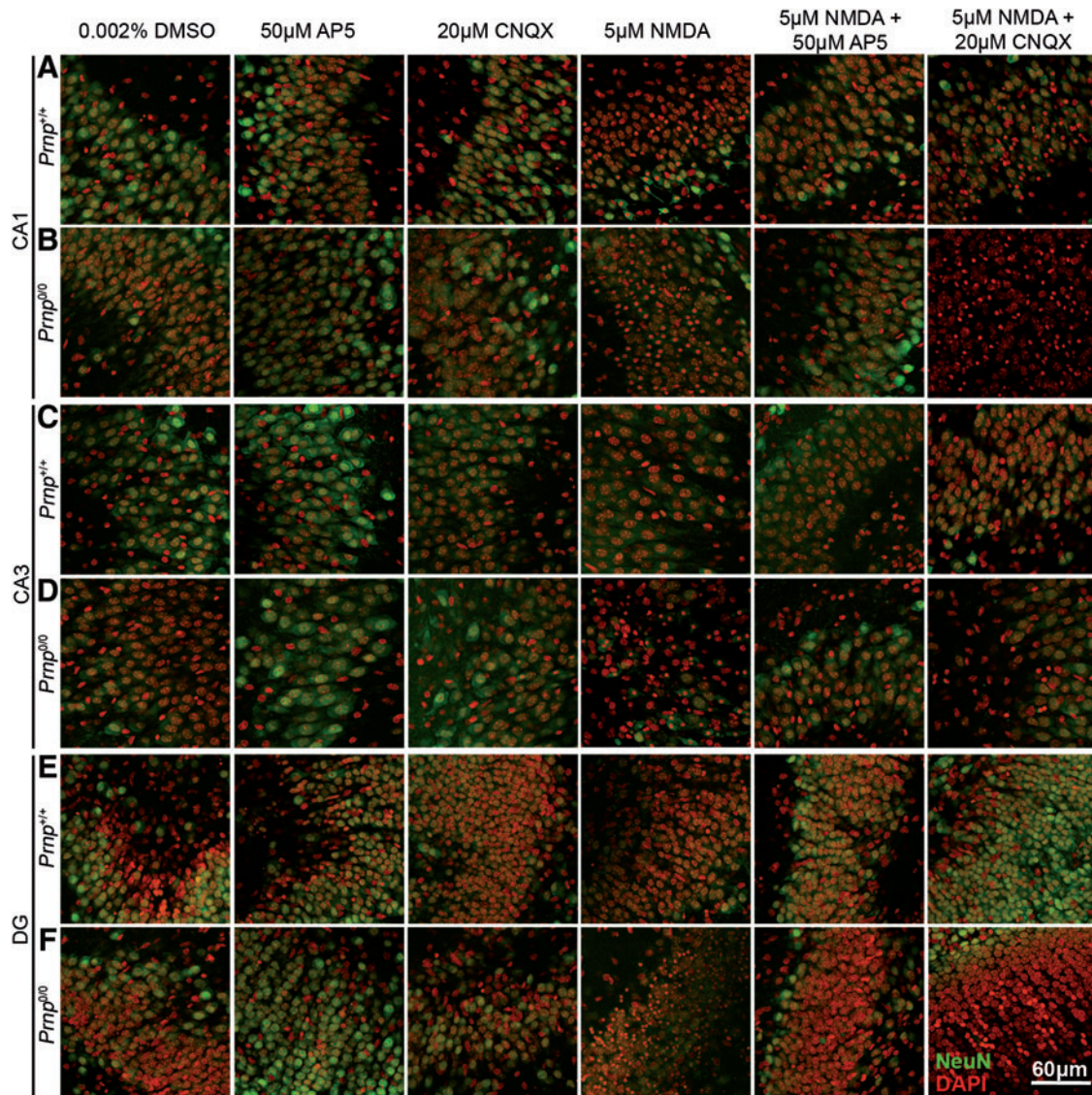


**SUPPLEMENTARY FIG. S4. The MTT assay confirms PrP<sup>C</sup>-null OHC higher susceptibility to excitotoxicity compared with wild-type OHC in the early phase after NMDA treatment.** The graph shows the cell viability percentage in *Prnp*<sup>+/+</sup> and *Prnp*<sup>0/0</sup> OHC treated and not treated with 5  $\mu$ M NMDA for 3 h; all bars indicate SD;  $n=12$ ; \*\* $p < 0.01$ . OHC, organotypic hippocampal cultures.

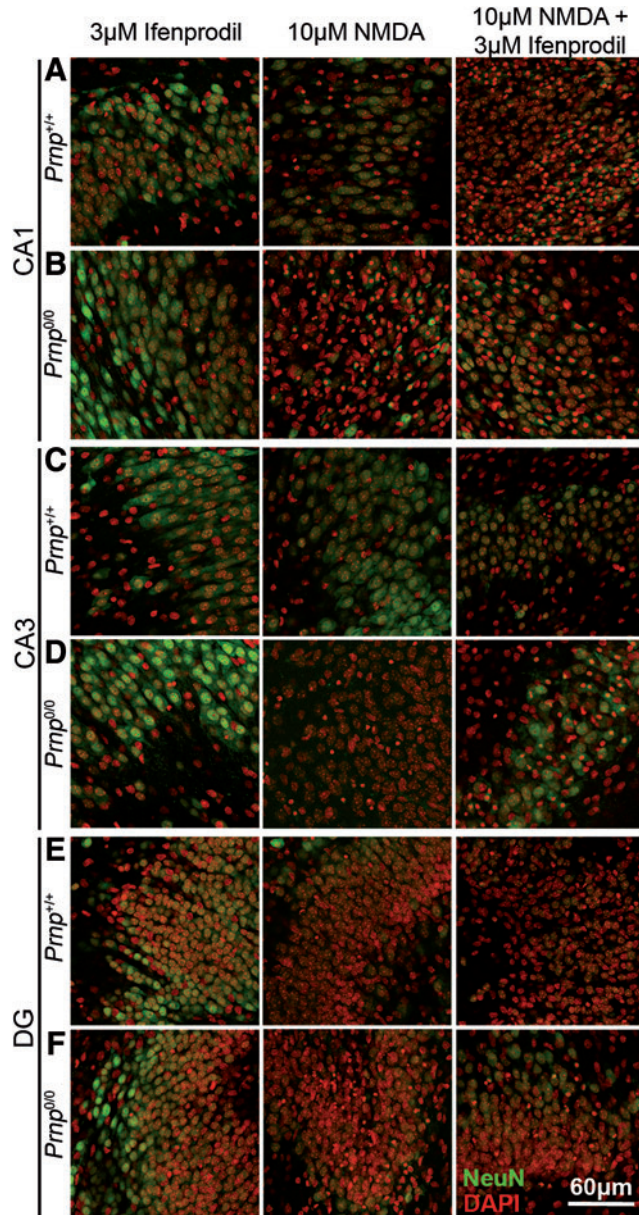


**SUPPLEMENTARY FIG. S5. Neuronal cell death induced by NMDA treatment is prevented by calcium chelation.** Images from *Prnp*<sup>+/+</sup> and *Prnp*<sup>0/0</sup> OHC areas are reported in rows: (A) *Prnp*<sup>+/+</sup> CA1; (B) *Prnp*<sup>0/0</sup> CA1; (C) *Prnp*<sup>+/+</sup> CA3; (D) *Prnp*<sup>0/0</sup> CA3; (E) *Prnp*<sup>+/+</sup> DG; (F) *Prnp*<sup>0/0</sup> DG. The different treatments are reported in columns: 2 mM EGTA for 1.5 h, first column; 5 μM NMDA for 1.5 h, second column; 5 μM NMDA+2 mM EGTA for 1.5 h, third column; 10 μM NMDA for 10 min, fourth column; 10 μM NMDA+2 mM EGTA for 10 min, fifth column. NeuN staining is displayed in green and DAPI in red. Confocal microscope fluorescence images were acquired using a 40×/1.30 NA oil objective. Comparison of neuronal pyknotic nuclei percentages induced by 10 μM NMDA for 10 min, between EGTA-treated *Prnp*<sup>+/+</sup> and *Prnp*<sup>0/0</sup> OHC in the (G) CA1, (H) CA3, and (I) DG; n=4 OHC, 5 slices per treatment in each culture; all error bars indicate SD; \*p<0.05. CA1, Cornus Ammonis 1; CA3, Cornus Ammonis 3; DAPI, 4',6-diamidino-2-phenylindole; DG, dentate gyrus; EGTA, ethylene glycol tetraacetic acid.

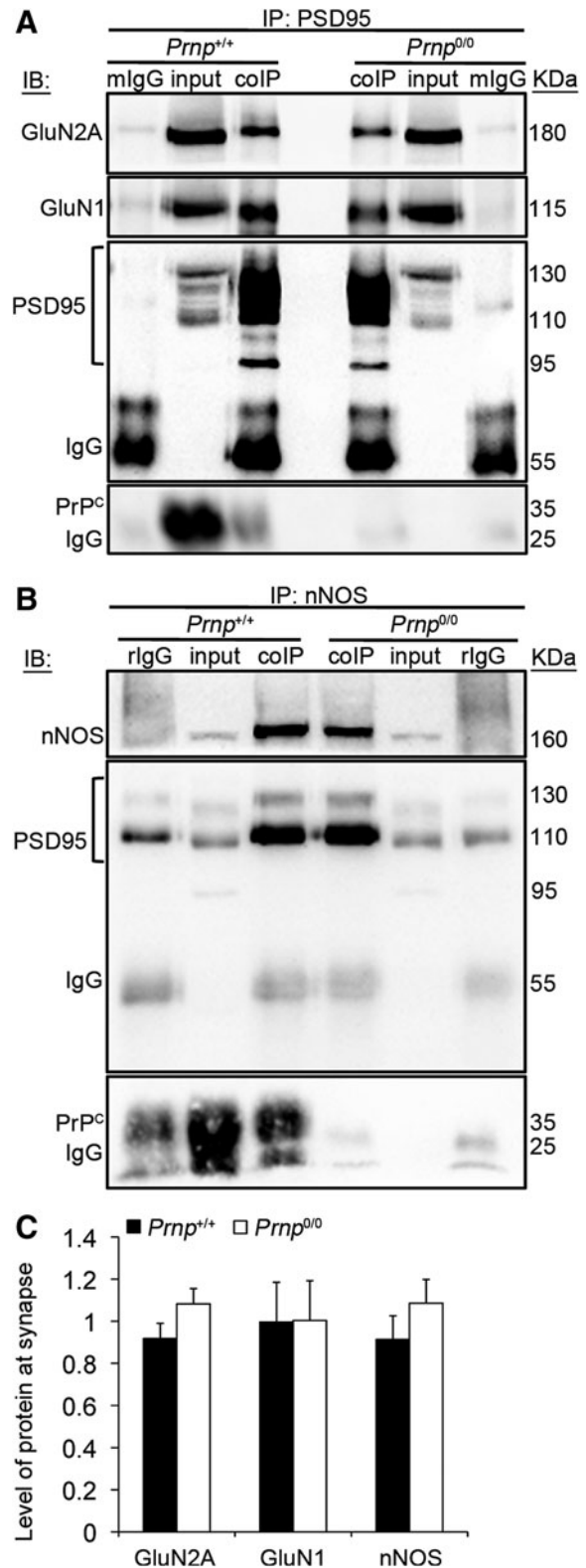




**SUPPLEMENTARY FIG. S6. Neuronal cell death induced by NMDA treatment is prevented by NMDAR antagonist and unaltered by AMPA/kainate receptor antagonist.** Images from *Prnp*<sup>+/+</sup> and *Prnp*<sup>0/0</sup> OHC areas are reported in rows: (A) *Prnp*<sup>+/+</sup> CA1; (B) *Prnp*<sup>0/0</sup> CA1; (C) *Prnp*<sup>+/+</sup> CA3; (D) *Prnp*<sup>0/0</sup> CA3; (E) *Prnp*<sup>+/+</sup> DG; (F) *Prnp*<sup>0/0</sup> DG. The different treatments are reported in columns: 0.002% DMSO for 3 h, *first column*; 50  $\mu$ M AP5 for 3 h, *second column*; 20  $\mu$ M CNQX for 3 h, *third column*; 5  $\mu$ M NMDA for 3 h, *fourth column*; 5  $\mu$ M NMDA + 50  $\mu$ M AP5 for 3 h, *fifth column*; 5  $\mu$ M NMDA + 20  $\mu$ M CNQX for 3 h, *sixth column*. NeuN staining is displayed in *green* and DAPI in *red*. Confocal microscope fluorescence images were acquired using a 40 $\times$ /1.30 NA oil objective. AMPA,  $\alpha$ -amino-3-hydroxy-5-methyl-4-isoxazolepropionic acid; AP5, (2*R*)-amino-5-phosphonovaleric acid; CNQX, 6-cyano-7-nitroquinoxaline-2,3-dione; DMSO, dimethyl sulfoxide.

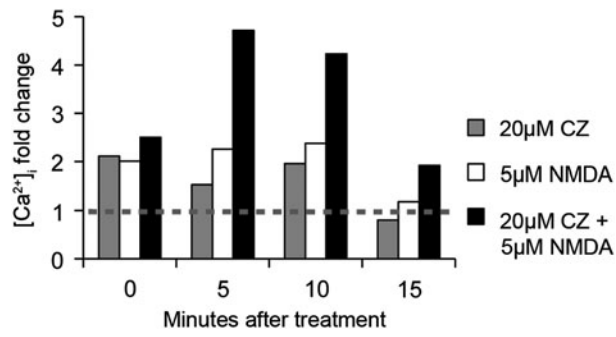


**SUPPLEMENTARY FIG. S7. Neuronal cell death induced by NMDA treatment is unaltered by GluN2B-containing NMDAR antagonist.** Images from *Prnp*<sup>+/+</sup> and *Prnp*<sup>0/0</sup> OHC areas are reported in rows: (A) *Prnp*<sup>+/+</sup> CA1; (B) *Prnp*<sup>0/0</sup> CA1; (C) *Prnp*<sup>+/+</sup> CA3; (D) *Prnp*<sup>0/0</sup> CA3; (E) *Prnp*<sup>+/+</sup> DG; (F) *Prnp*<sup>0/0</sup> DG. The different treatments are reported in columns: 3 μM Ifenprodil for 10 min, left column; 10 μM NMDA for 10 min, central column; 5 μM NMDA + 3 μM Ifenprodil for 10 min, right column. NeuN staining is displayed in green and DAPI in red. Confocal microscope fluorescence images were acquired using a 40×/1.30 NA oil objective.

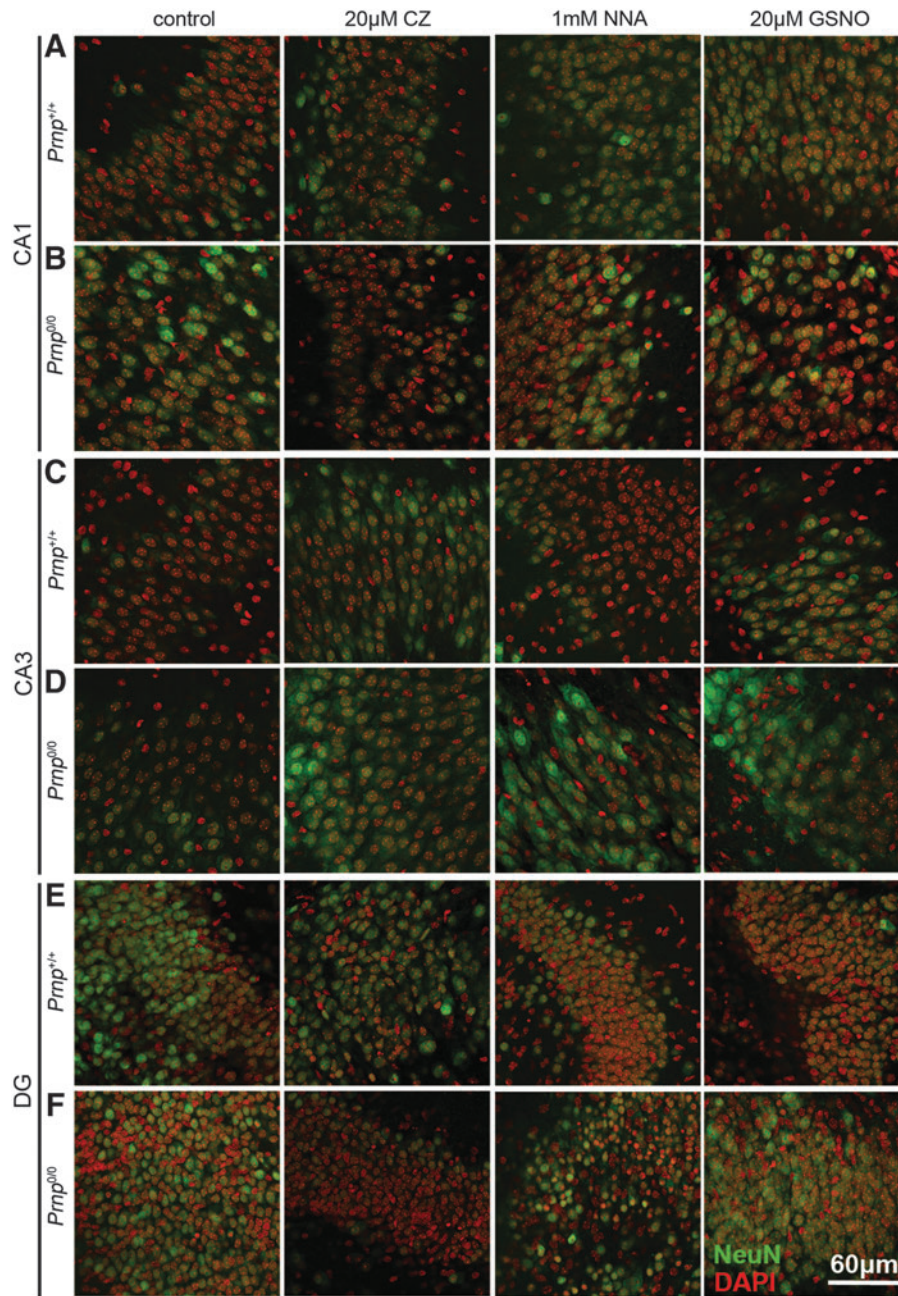


**SUPPLEMENTARY FIG. S8. CoIP of GluN2A and GluN1 with PSD95 and coIP of PSD95 with nNOS show comparable levels in P20 *Prnp*<sup>+/+</sup> and *Prnp*<sup>0/0</sup> hippocampi.** (A) coIP of GluN2A and GluN1 with PSD95. (B) coIP of PSD95 with nNOS. (C) Graph showing the quantification of the coIP signals normalized according to the following formula: (co-immunoprecipitated protein/input)/(immunoprecipitated protein/input); all error bars indicate SD; *n* = 3.

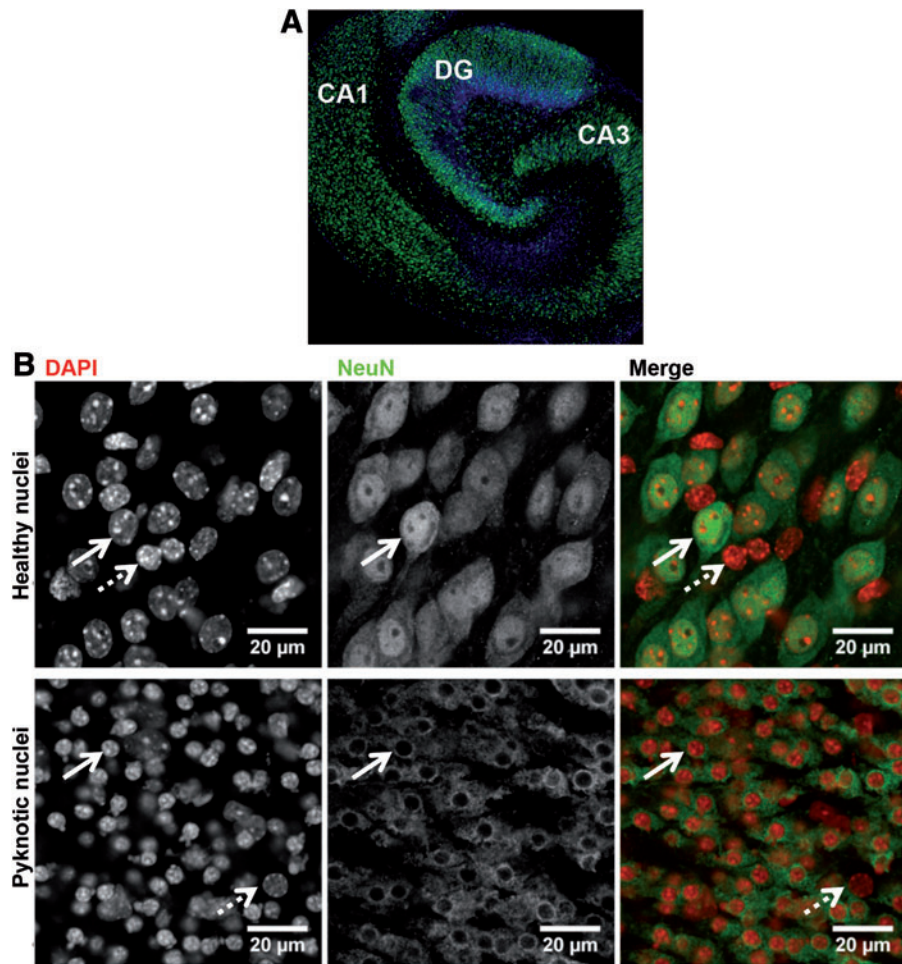




**SUPPLEMENTARY FIG. S9. Copper chelation increases NMDA-induced [Ca<sup>2+</sup>]<sub>i</sub> waves.** The graph shows fluorescence intensity subtracted of the background intensity and normalized on resting condition measurements. The *dashed line* indicates the untreated cell fluorescence.



**SUPPLEMENTARY FIG. S10. Treatments with CZ, NNA, and GSNO do not affect neuron health.** Images from *Prmp*<sup>+/+</sup> and *Prmp*<sup>0/0</sup> OHC areas are reported in rows: (A) *Prmp*<sup>+/+</sup> CA1; (B) *Prmp*<sup>0/0</sup> CA1; (C) *Prmp*<sup>+/+</sup> CA3; (D) *Prmp*<sup>0/0</sup> CA3; (E) *Prmp*<sup>+/+</sup> DG; (F) *Prmp*<sup>0/0</sup> DG. The different treatments are reported in columns: control, first column; 20  $\mu$ M CZ for 3 h, second column; 1 mM NNA for 3 h, third column; 20  $\mu$ M GSNO for 3 h, fourth column. NeuN staining is displayed in green and DAPI in red. Confocal microscope fluorescence images were acquired using a 40 $\times$ /1.30 NA oil objective. CZ, cuprizone; GSNO, S-nitrosoglutathione.



**SUPPLEMENTARY FIG. S11. Description of the OHC system.** (A) OHC staining with DAPI (in *red*) and anti-NeuN antibody (in *green*). Confocal microscope fluorescence images were acquired using a  $10\times/0.30$  NA dry objective. (B) Example of discrimination between healthy and pyknotic neuronal nuclei. Neurons are indicated by *white arrows*, while glia cells are indicated by *dashed arrows*. DAPI is displayed in *red* and anti-NeuN antibody staining in *green*. Confocal microscope fluorescence images were acquired using a  $63\times/1.40$  NA oil objective.